OPAL Physics Note PN089
9 January 1993

Measurement of the B^0 and B^+ lifetimes

The OPAL Collaboration

Abstract

From a data sample of approximately 240 000 hadronic Z^0 decays recorded during 1991 a sample of about 130 semi-leptonic B hadron decays containing a D^0, D^+ or D^{*+} has been isolated. Using silicon microvertex detector information the decay vertices in these events have been reconstructed. The average B hadron lifetime of this event sample is measured to be $1.51^{+0.16+0.11}_{-0.14-0.11}$ ps. From the distribution of decay times in the different samples the lifetimes of the B^0 and B^+ mesons are determined to be $1.51^{+0.24+0.11}_{-0.23-0.13}$ ps and $1.52^{+0.29+0.11}_{-0.27-0.12}$ ps respectively. The measured ratio of the B^+ to B^0 lifetimes of $1.01^{+0.32+0.06}_{-0.24-0.07}$ confirms expectations that the lifetimes are similar.

1 Introduction

Measurements of the average[1] B lifetime with data from the LEP experiments [1] have already reached a precision where sensitivity to variations between the different weakly decaying species is important. The measurement of the individual B lifetimes tests the validity of the spectator model for B hadrons. Any variations are expected to be limited to the 10% level [2]. Furthermore, because the B hadron lifetimes are used to determine the Cabibbo-Kobayashi-Maskawa matrix elements governing the b quark couplings to the first and second generations of quarks, a large deviation from the spectator model would be important. It is therefore of interest to measure the lifetimes of the different B hadron species, which can be separated by reconstructing B hadrons in (semi-)exclusive decay modes. Using the current OPAL data, the most experimentally accessible channels are semi-leptonic decays with a fully reconstructed charm hadron, *e.g.*:

$$\mathrm{B} \to \overline{\mathrm{D}}^0 \ell^+ \mathrm{X}, \quad \mathrm{B} \to \mathrm{D}^- \ell^+ \mathrm{X}, \quad \mathrm{B} \to \mathrm{D}^{*-} \ell^+ \mathrm{X}, \quad \mathrm{B}_s \to \mathrm{D}_s^- \ell^+ \mathrm{X}, \quad \Lambda_b \to \Lambda_c^+ \ell^- \mathrm{X}$$

where ℓ^+ is either an electron or muon. Charge conjugation is implicitly assumed throughout this letter. The first three decay modes are expected to allow partial separation of B^+ and B^0, whilst the others have already been used by OPAL to provide clear signatures for B_s and Λ_b production [3, 4].

In this letter we report on an analysis using precision tracking provided by our silicon microvertex detector to reconstruct the individual charm and bottom hadron decay vertices in semi-leptonic B decays. We calculate the decay time for each B hadron using its measured decay length and estimated energy. We use the resulting decay times to measure the exclusive B hadron lifetimes. Results are presented for the B^0 and B^+ lifetimes using our 1991 data.

2 The OPAL detector

A complete description of the OPAL detector can be found elsewhere [5, 6]. We describe briefly the aspects of the detector pertinent to this analysis. Tracking of charged particles is performed by the central detector consisting of a large volume jet chamber, a precision vertex drift chamber and chambers measuring the z-coordinate[2] of tracks as they leave the jet chamber. For the 1991 LEP run this tracking system was enhanced by the addition of a silicon microvertex (μVTX) detector. The central detector is positioned inside a solenoidal coil which provides a uniform magnetic field of 0.435 T. The momentum resolution obtained is approximately $\sigma_{p_{xy}}/p_{xy} = \sqrt{(0.02)^2 + (0.0015 p_{xy})^2}$, where p_{xy} is in GeV. In addition to tracking charged particles, the jet chamber provides measurements of the ionisation loss of charged particles, which are used for particle identification. The coil is surrounded by a time-of-flight counter array and a lead-glass electromagnetic calorimeter with presampler. Outside the electromagnetic calorimeter is the instrumented return yoke of the magnet, which forms the hadron calorimeter. This is surrounded by muon chambers.

Crucial to this analysis is the μVTX detector [6]. This detector consists of two concentric arrays of silicon strip detectors at radii of 6.1 cm and 7.5 cm surrounding a 5.3 cm radius beryllium beampipe. Each silicon wafer has 629 readout strips with a pitch of 50 μm. Between

[1] Most of the average B hadron lifetime measurements utilize inclusive semi-leptonic decays and therefore more closely measure a mean weighted by relative production rates and semi-leptonic branching fractions.

[2] The OPAL coordinate system is defined with positive z being along the electron beam direction, θ and ϕ being the polar and azimuthal angles respectively.

each of these is an additional p^+ implant which linearises the charge division. The detector has an active length of 18 cm, giving two layer acceptance for $|\cos\theta| < 0.76$. The efficiency for reconstructing a hit within the detector fiducial region has been determined to be greater than 0.97 using $Z^0 \to \mu^+\mu^-$decays. The detectors provide $r-\phi$ hit coordinates with an intrinsic precision better than 6 μm. However, alignment uncertainties within OPAL currently limit the space-point resolution to about 10 μm. When combined with the angle and curvature information provided by the other central detector components this results in an impact parameter resolution of 18 μm for tracks in $Z^0 \to \mu^+\mu^-$and $Z^0 \to e^+e^-$events.

3 Particle identification

Charged pions and kaons are identified using dE/dx information from the jet chamber [7]. For the momentum region between 2 GeV and 20 GeV the separation between pions and kaons is greater than two standard deviations. We consider a particle to be consistent with a specific hypothesis if the probability for the measured dE/dx value is calculated to be greater than 1%. For kaons, if the measured dE/dx is higher than the expected value, we tighten this requirement to 3%.

The electron identification procedure used in this analysis is the same as that described in a previous publication [8] and covers the angular range $|\cos\theta| < 0.70$. It uses the dE/dx measured in the jet chamber, shower shape information from the electromagnetic calorimeter and presampler, and the quantity E_{cal}/p, where E_{cal} is the energy deposited in the calorimeter around the extrapolated position of the central detector track of momentum p. Futhermore, electron candidates which are identified as arising from photon conversions are rejected. In the kinematic range relevant to this analysis the electron identification efficiency is about 55%. The probability to misidentify a hadron as an electron is of the order 0.1%.

Muons are identified by associating central detector tracks with track segments in the muon chambers, requiring a position match in two orthogonal coordinates. In addition, loose requirements on dE/dx are made to reject kaons and protons. The average identification efficiency is approximately 75% for muons with $p > 3$ GeV and $|\cos\theta| < 0.90$. Hadrons may fake muons either by being misidentified or by decaying in flight to muons. The average probability for a hadron to fake a prompt muon in this kinematic range is estimated to be 0.8%.

4 Event selection

This analysis is based on about 11.1 pb^{-1} of data recorded in 1991 after the μVTX detector was commissioned. The data were collected from e^+e^- annihilations at centre of mass energies between 88.5 and 93.8 GeV. The selection criteria for hadronic Z^0 decays are described elsewhere [9]. The efficiency of the hadronic selection criteria is determined to be (98.4 ± 0.4)%. After data quality and detector performance requirements, the available data sample consists of about 240 000 events.

The selection of $B \to \overline{D}\ell^+X$ events uses both the kinematic and vertex information of the decays. In table 1 we summarize the selection criteria for the four different decay modes which we consider. The kinematic selection is similar to those used in previous OPAL analyses [3, 4]. D mesons are selected by considering all track combinations consistent with the appropriate particle identification hypotheses. To reduce combinatorial background D meson candidates are required to have a minimum energy (E_D) in the range 5–9 GeV depending on the decay mode.

Decay mode	E_{D} (GeV)	p_{K} (GeV)	p_π (GeV)	$\mid \cos\theta^* \mid$	$m_{\mathrm{D}\ell}$ (GeV)	$E_{\mathrm{D}\ell}$ (GeV)	l_{D}/σ_l
$\mathrm{D}^0 \to \mathrm{K}^-\pi^+$	> 6	> 2	> 1	< 0.8	> 3.0	> 13.5	> -1
$\mathrm{D}^+ \to \mathrm{K}^-\pi^+\pi^+$	> 9	> 2	> 0.8	< 0.8	> 3.2	> 13.5	> -1
$\mathrm{D}^{*+} \to \mathrm{D}^0\pi^+$, $\mathrm{D}^0 \to \mathrm{K}^-\pi^+$	> 5	> 0.15	> 0.15	< 0.95	> 2.8	> 9.0	-
$\mathrm{D}^{*+} \to \mathrm{D}^0\pi^+$, $\mathrm{D}^0 \to \mathrm{K}^-\pi^+\pi^+\pi^-$	> 9	> 2	> 0.5	-	> 3.0	> 13.5	-

Table 1: Decay mode dependent selection criteria.

To select D^{*+} candidates we require a π^+ in addition to a D^0 candidate. The difference between the mass of the D^{*+} candidate and that of the D^0 is required to be in the range 0.142–0.148 GeV. To further reduce the background we require the momenta of the decay products (p_{K}) and (p_π) to satisfy minimum momenta criteria. For some decay modes we also cut on $\cos\theta^*$, where θ^* is the angle between the K^- and the D boost direction in the D rest frame. For the D^+ candidates we also require that the mass of each $\mathrm{K}^-\pi^+$ combination be less than 1.55 GeV. This cut rejects partially reconstructed D^0 decays which form a peak at about 1.6 GeV and could fake a D^+ if combined with a pion from a $\mathrm{D}^{*+} \to \mathrm{D}^0\pi^+$ decay.

Lepton candidates are required to have $p > 2$ GeV. All $\overline{\mathrm{D}}\ell^+$ combinations are considered as possible $\mathrm{B} \to \overline{\mathrm{D}}\ell^+$ candidates. To suppress random combinations we require the candidates to satisfy minimum mass (m_{Dl}) and energy (E_{Dl}) criteria. In addition all candidates are required to have $m_{Dl} < 5.35$ GeV. In order to select events suitable for lifetime determination, and to reduce the background further we make use of the vertex information.

In order to reject poorly determined and possibly badly reconstructed decays we require that the lepton track and at least two of the D decay tracks each be associated with at least one hit in the μVTX detector. This ensures that vertex reconstruction is dominated by the μVTX detector information. The association of μVTX hits to tracks found in the other central tracking components requires that $P(\chi^2)$ be greater than 0.1% for all matches. Using a simulation of the OPAL detector [10] the efficiency for matching tracks with two real hits in the μVTX detector was determined to be 96 %, whilst the fraction with wrongly assigned hits was found to be 2%. The corresponding fractions for tracks with one real μVTX hit are 93 % and 5% respectively.

To reconstruct the decay vertices we minimize the $\chi^2(x_B, y_B, l_D, k_1 \ldots k_i, \phi_1 \ldots \phi_i)$, where (x_B, y_B) are the coordinates of the B decay vertex, l_D is the decay length of the D meson and k_i and ϕ_i are the curvature and angle of the i^{th} track at the relevant decay vertex. The direction of flight of the D meson is fixed to correspond to its momentum vector. We demand that $P(\chi^2)$ for the vertex fit be greater than 1% in order to suppress fake track combinations and badly reconstructed vertices. The B hadron decay length is calculated in the $r - \phi$ plane using the

Decay mode	Number of candidates	Estimated Background	signal
$D^0 \to K^-\pi^+$	96	26	70 ± 10
$D^+ \to K^-\pi^+\pi^+$	62	20	42 ± 8
$D^{*+} \to D^0\pi^+$, $D^0 \to K^-\pi^+$	28	5	23 ± 5
$D^{*+} \to D^0\pi^+$, $D^0 \to K^-\pi^+\pi^+\pi^-$	20	7	13 ± 4

Table 2: Number of events and background for each decay mode.

position of the reconstructed $\overline{\mathrm{D}}\ell^+$ vertex and the average e^+e^- interaction point. The B decay length is signed according to the cosine of the angle between the $\overline{\mathrm{D}}\ell^+$ momentum vector and the decay direction. To convert the decay length into three dimensions we estimate $\sin\theta$ for the B hadron from the $\overline{\mathrm{D}}\ell^+$ momentum vector. The B hadrons have typical decay lengths of 2.9 mm and are reconstructed with a resolution of about 300 μm. We require the error on the B decay length to be less than 5 mm to reject a small fraction of badly reconstructed decays. As the reconstructed D decay length (l_{D}) is independent of the B hadron production point and therefore also of the B hadron decay length, we can use this to reject background. For all decay modes we require $|l_{\mathrm{D}}| < 1$ cm. For the inclusive D^0 and D^+ samples we make a cut on the decay length significance (l_{D}/σ_l), where σ_l is the resolution on l_{D}.

The resulting signals for the four different decay modes together with the corresponding $\overline{\mathrm{D}}\ell^-$ combinations are shown in figures 1 and 2. A clear signal is visible in each of these decay modes. No significant signals are observed in the $\overline{\mathrm{D}}\ell^-$ combinations, indicating a negligible contribution from D mesons combined with fake leptons. The $K^-\pi^+$ mass distributions also show indications of a peak around 1.6 GeV. An enhancement is expected in this region from the decays $D^0 \to K^-\pi^+\pi^0$, in which the π^0 is not reconstructed. A similar, but broader enhancement is seen in the $K^-\pi^+\pi^+$ mass distribution. Our simulation indicates that we should expect appreciable contributions from the decays $D^0 \to K^-\pi^+\pi^+\pi^-$ and $D^+ \to K^-\pi^+\pi^+\pi^0$. We have determined the signal and background in each channel by fitting the mass distributions using a function consisting of a sum of Gaussians and a second order polynomial background term. The widths of the signal Gaussians are determined from a full simulation of the OPAL detector [10]. The enhancements around 1.6 GeV are also parameterized as Gaussians and included in the fit.

For the lifetime determinations we select candidates in the mass range ± 60 MeV around the nominal D meson masses [11]. The resulting signals and estimated backgrounds are listed in table 2. In order to have statistically independent samples for the lifetime analysis we remove 14 events from the $D^0 \to K^-\pi^+$ sample which are also identified as D^{*+} candidates.

5 Lifetime fitting

In order to convert the measured decay lengths into decay times it is necessary to estimate the energy of the B hadrons. We do this by using the kinematics of the B hadron decays to

correct for the missing energy on an event-by-event basis. By using this method we effectively eliminate any dependence of the decay time distribution on the b quark fragmentation function. In order to estimate the B hadron energy (E) from the observed decay products we use the following estimator:

$$E = \frac{E_{Dl} \cdot m_B}{m_{Dl}}(1 + a_1\Delta m + a_2\Delta m^2) \tag{1}$$

where $\Delta m = (m_B - m_{Dl})/m_B$ for $m_{Dl} < m_B$ and $\Delta m = 0$ for $m_{Dl} > m_B$. The constants a_1 and a_2 may depend on the decay mode and any selection criteria applied. We have determined these constants individually, for each decay mode of interest, using simulated event samples selected with the same criteria as used for the data. Typical values are $a_1 = 0.02$ and $a_2 = -0.80$. Our simulation indicates that this method of correcting for the missing energy is independent of the B energy spectrum and hence of uncertainties in the fragmentation function.

In addition to the B energy, we also estimate its uncertainty on an event-by-event basis. The width of the energy resolution function has a strong dependence on the visible mass (m_{Dl}). We use the form:

$$\sigma_E/E = b_0 + b_1\Delta m \tag{2}$$

Typical values are $b_0 = 0.025$ and $b_1 = 0.40$ corresponding to $\sigma_E/E \sim 8\%$ for $m_{Dl} = 4.5$ GeV and $\sigma_E/E \sim 21\%$ for $m_{Dl} = 3$ GeV.

Using the individual decay length and energy estimates we calculate the decay time (t_i) for each B $\to \overline{\mathrm{D}}\ell^+$ candidate and use a maximum likelihood fit to extract the B hadron lifetimes. The B decay time distributions ($\mathcal{F}_B$) are expected to be exponentials convoluted with Gaussian resolution functions. For each candidate the resolution on the decay time is given by:

$$\frac{\sigma_{t_i}^2}{t_i^2} = \frac{\sigma_{l_i}^2}{l_i^2} + \frac{\sigma_E^2}{E^2} \tag{3}$$

where σ_{l_i} is the error on the decay length. The decay time resolution receives roughly equal contributions from each source.

To take into account the background when fitting for the lifetimes we have studied samples selected outside the signal regions and in the $\overline{\mathrm{D}}\ell^-$ events. We find that in all cases the average apparent lifetime of these samples is close to zero. As a result we have parameterized the background lifetime distributions as the sum of two Gaussians:

$$\mathcal{F}_{back} = \frac{c_1}{\sigma_i\sqrt{2\pi}}\exp(\frac{-{t_i}^2}{2{\sigma_i}^2}) + \frac{1-c_1}{\sqrt{{\sigma_i}^2+{c_2}^2}\sqrt{2\pi}}\exp(\frac{-(t_i-c_3)^2}{2({\sigma_i}^2+{c_2}^2)}) \tag{4}$$

where $\sigma_i^2 = \sigma_{l_i} \cdot t_i/l_i$ is the expected measurement resolution. The second Gaussian is intended to include any residual lifetime information in the background. The constants c_1, c_2 and c_3 are determined by fitting the background samples. All the fits give consistent results and indicate that about half of the background is described by the first Gaussian in equation 4, corresponding to the resolution function. The remainder is described by a broad Gaussian of width ~ 2 ps. This contribution represents the various random combinations of B tracks combined with unrelated tracks. Since the different background samples yield similar results we use a fit to a combined sample to describe the background in all channels.

In order to determine the lifetime from each of the samples we use a likelihood function of the form:

$$\mathcal{F} = f \cdot \mathcal{F}_B + (1-f) \cdot \mathcal{F}_{back} \tag{5}$$

Decay mode	Fitted lifetime (ps)
$D^0 \to K^-\pi^+$	$1.54^{+0.25}_{-0.21}$
$D^+ \to K^-\pi^+\pi^+$	$1.30^{+0.27}_{-0.22}$
$D^{*+} \to D^0\pi^+$, $D^0 \to K^-\pi^+$	$1.71^{+0.45}_{-0.34}$
$D^{*+} \to D^0\pi^+$, $D^0 \to K^-\pi^+\pi^+\pi^-$	$1.67^{+0.61}_{-0.42}$
Combined D^{*+}	$1.70^{+0.35}_{-0.27}$
Combined sample	$1.51^{+0.16}_{-0.14}$

Table 3: Lifetime fit results for different $\overline{\mathrm{D}}\ell^+$ samples.

where the signal fractions (f) are as determined in section 4 (see table 2).

Figure 3 shows the resulting fits to the data for the three different decay modes that we have considered. The resulting lifetimes are summarized in table 3. All the lifetime measurements are consistent. The average B hadron lifetime determined from the combined sample is $\langle\tau\rangle = 1.51^{+0.16}_{-0.14}$ ps.

6 Determination of the B^0 and B^+ lifetimes

The different samples of $\overline{\mathrm{D}}\ell^+$ events are expected to contain different fractions of B^0 and B^+ decays. The primary sources of these events are expected to be the semi-leptonic decays of B^0 and B^+ mesons to pseudo-scalar, vector and p-wave charmed mesons (the so-called D^{**}'s):

$$\begin{array}{lll} B^0 \to D^-\ell^+\nu, & B^0 \to D^{*-}\ell^+\nu, & B^0 \to D^{**-}\ell^+\nu, \\ B^+ \to \overline{D}^0\ell^+\nu, & B^+ \to \overline{D}^{*0}\ell^+\nu, & B^+ \to \overline{D}^{**0}\ell^+\nu. \end{array}$$

We use the symbol D^{**} to represent, in addition to the p-wave states, possible non-resonant decays of the type $B \to \overline{D}(n\pi)\ell^+X$ and higher spin states. Decays of the B_s and Λ_b to final states containing a $\overline{D}^{(*)}\ell^+$ combination *e.g.* $B_s \to D^*_{s1}(2536)^-\ell^+\nu$, $D^*_{s1}(2536)^- \to D^*\overline{K}^0$, are expected to be completely negligible within the current statistics unless the lifetimes of the B_s and Λ_b differ significantly from those of the B^0 or B^+.

In the absence of any D^{**} decays the states containing a $D^-\ell^+$ and D^{*-} would be almost completely B^0. If we assume that the production rates of the B^0 and B^+ mesons are equal then with the addition of possible D^{**} decays the relative fractions in each of the samples may be expressed as follows:

$$\begin{aligned} \mathcal{R}\left(\frac{B^0 \to \overline{D}^0\ell^+X}{B^+ \to \overline{D}^0\ell^+X}\right) &= \frac{\tau^0}{\tau^+}\frac{g^{00}}{g^{+0}}, \\ \mathcal{R}\left(\frac{B^0 \to D^-\ell^+X}{B^+ \to D^-\ell^+X}\right) &= \frac{\tau^0}{\tau^+}\frac{g^{0+}}{g^{++}}, \end{aligned} \qquad (6)$$

$$\mathcal{R}\left(\frac{\mathrm{B}^0 \to \mathrm{D}^{*-}\ell^+\mathrm{X}}{\mathrm{B}^+ \to \mathrm{D}^{*-}\ell^+\mathrm{X}}\right) = \frac{\tau^0}{\tau^+}\frac{g^{0*}}{g^{+*}},$$

where,

$$\begin{aligned}
g^{00} &= (1-\eta^*)b^0 f^* + \frac{2}{3}f^{**} + \frac{1}{3}(1-\eta^*)b^0 p_v f^{**}, \\
g^{+0} &= f^0 + f^* + \frac{1}{3}f^{**} + \frac{2}{3}(1-\eta^*)b^0 p_v f^{**}, \\
g^{0+} &= f^0 + (1-b^0)f^* + \frac{1}{3}(1-p_v)f^{**} + \frac{1}{3}(1-b^0)p_v f^{**}, \\
g^{++} &= \frac{2}{3}(1-b_0)p_v f^{**} + \frac{2}{3}(1-p_v)f^{**}, \\
g^{0*} &= f^* + \frac{1}{3}p_v f^{**}, \\
g^{+*} &= \frac{2}{3}p_v f^{**}.
\end{aligned}$$

Here we have assumed that the D^{**} decays are dominated by the modes $\mathrm{D}^{**} \to \mathrm{D}^{(*)}\pi$ and have used isospin to determine the relative fractions of the decays yielding charged and neutral $\mathrm{D}^{(*)}$'s. The relative fractions of B^0 or B^+ in the samples depend on their lifetimes, τ^0 and τ^+. This arises because the semi-leptonic decays are pure spectator processes, hence their widths are expected to be constant, irrespective of any variation in the lifetimes. For b^0, the branching ratio $B(\mathrm{D}^{*+} \to \mathrm{D}^0\pi^+)$, we use the recent CLEO [12] measurement of 0.68 ± 0.03. The relative efficiency (η^*) for reconstruction a D^{*+}, after reconstructing a D^0 is found from our simulation to be $\eta^* = 0.76 \pm 0.03$.

The quantities f^0, f^* and f^{**} are the fraction of the semi-leptonic decays resulting in a D, D^* or D^{**} respectively. These are assumed to be the same for B^0 or B^+. In equation 6 we have implicitly assumed that the reconstruction efficiencies for a particular $\mathrm{B} \to \overline{\mathrm{D}}^{(*)}\ell^+\mathrm{X}$ decay are independent of the exclusive B decay mode. The corrections due to the differences in the relative efficiencies are small. Using our simulation we find them to be in the range 0.94-1.00 for the $\mathrm{B} \to \overline{\mathrm{D}}^*\ell^+\nu$ decays and in the range 0.77-0.95 for the $\mathrm{B} \to \overline{\mathrm{D}}^{**}\ell^+\nu$ decays. The exclusive semi-leptonic branching ratios of B^0 or B^+ to pseudo-scalar and vector states have been measured at the $\Upsilon(4\mathrm{S})$ [13, 14, 15]. We average the CLEO [14] and ARGUS measurements [15] to obtain $f^{**} = 0.29 \pm 0.07$. We combine this number with the exclusive branching ratios [11], averaged over charged and neutral states to obtain:

$$\begin{aligned}
f^0 &= \frac{B(\mathrm{B} \to \overline{\mathrm{D}}\ell^+\nu)}{B(\mathrm{B} \to \overline{\mathrm{D}}\ell^+\nu) + B(\mathrm{B} \to \overline{\mathrm{D}}^*\ell^+\nu)}(1-f^{**}) = 0.18, \\
f^* &= \frac{B(\mathrm{B} \to \overline{\mathrm{D}}^*\ell^+\nu)}{B(\mathrm{B} \to \overline{\mathrm{D}}\ell^+\nu) + B(\mathrm{B} \to \overline{\mathrm{D}}^*\ell^+\nu)}(1-f^{**}) = 0.53.
\end{aligned}$$

The fractions of B^0 and B^+ in the event samples are insensitive to the ratio f^0/f^* so only variations in f^{**} are considered when evaluating the uncertainty in the sample compositions. The variation of the fraction of B^0 in the different $\overline{\mathrm{D}}\ell^+$ samples is shown in figure 4a.

The remaining unknown p_v is the fraction of D^{**} decays to a vector (as opposed to a pseudo-scalar) charmed meson. In order to estimate p_v one needs to estimate the relative production rates and branching fractions of the different p-wave states. Estimates of p_v are not particularly sensitive to any reasonable assumptions about the production rates. We combine the predictions

of the relative production rates from [16] with predictions [17] and measurements [11] of the branching ratios to obtain $p_v = 0.54$. This value is consistent with the ARGUS data [15] which suggest that a significant fraction of the neutral D**'s are the $J^P = 1^+$ and 2^+ states $D_1(2420)^0$ and $D_2^*(2460)^0$. In figure 4b we show the variation of the fractions of B^0 in the samples as function of p_v. We have taken $p_v = 0.54$, but allow variations of ± 0.3 when considering uncertainties in the sample compositions.

In order to fit for τ^0 and τ^+ we carry out a maximum likelihood fit to the combined sample of $\overline{D}\ell^+$ events. The likelihood function given in equation 5 is modified to become the sum of two exponentials convoluted with Gaussians where the relative weight is determined by the assigned probability of a particular event being B^0 or B^+, according to equation 6. We have carried out a simulation to verify that we are able to determine the different individual lifetimes from a combined fit. A Monte Carlo sample was generated with $\tau^0 = 1.2$ ps and $\tau^+ = 1.6$ ps. The B decays were modelled with $f^{**} = 0.36$ and $p_v = 0.54$. The maximum likelihood fit results are shown in figure 5. The fit gives $\tau^0 = 1.169 \pm 0.046$ ps and $\tau^+ = 1.541 \pm 0.036$ ps in good agreement with the generated values. The incomplete separation between the B^0 and B^+ mesons in the $\overline{D}\ell^+$ samples results in a significant increase in the statistical error because of correlations between the lifetime functions.

We have carried out a maximum likelihood fit to the complete $\overline{D}\ell^+$ data sample, as shown in figure 6. The fit result is:

$$\tau^0 = 1.51^{+0.24}_{-0.23} \text{ ps},$$

$$\tau^+ = 1.52^{+0.29}_{-0.27} \text{ ps}.$$

We have also fitted directly the lifetime ratio and obtain $\tau^+/\tau^0 = 1.01^{+0.32}_{-0.24}$.

7 Systematic uncertainties

In order to evaluate the uncertainties in the sample compositions we allow f^{**} to vary by ± 0.14 and p_v to vary by ± 0.30. These variations have been conservatively chosen to cover all reasonable values for these parameters.

To estimate the uncertainties due to the background fractions and the apparent background lifetimes we have varied the parameters c_1 and c_3, which determine the decay time distribution, by $\pm 2\sigma$. We have also varied the total background fractions in each of the samples independently by $\pm 1\sigma$. Finally we have considered the extreme case of changing the background fractions in all samples by $\pm 1\sigma$ simultaneously.

We have investigated possible biases in the energy estimator (equation 1) by looking separately at Monte Carlo samples of D, D* and D** decays. The maximum difference is 2.7% which we consider as a possible systematic uncertainty. The energy resolution is well described by a Gaussian at the 10% level, however, we consider 20% variations in its value.

We have also considered possible detector effects. To allow for uncertainties in the detector resolutions we have considered variations of $\pm 20\%$ in the decay length resolutions. As a further check we have repeated the maximum likelihood fit with a fitted global error scale factor (k) multiplying the σ_{l_i} in equation 3. The fit yields $\tau^0 = 1.49^{+0.24}_{-0.23}$ ps, $\tau^+ = 1.51^{+0.29}_{-0.27}$ ps and $k = 1.08^{+0.28}_{-0.28}$, indicating that our tracking errors are well understood. We have also studied the effects of possible systematic biases in the track reconstruction due to misalignment of the μVTX detector. Because of the limited statistics of the B decay sample we have used

Systematic source	τ^0 (ps)	τ^+ (ps)	τ^+/τ^0	$\langle\tau\rangle$ (ps)
f^{**} ± 0.14	$^{+0.01}_{-0.01}$	$^{+0.01}_{-0.01}$	$^{+0.01}_{-0.01}$	-
p_v ± 0.30	$^{+0.02}_{-0.02}$	$^{+0.02}_{-0.02}$	$^{+0.03}_{-0.03}$	-
Background	$^{+0.04}_{-0.09}$	$^{+0.05}_{-0.08}$	$^{+0.05}_{-0.06}$	$^{+0.05}_{-0.06}$
Energy Estimator	$^{+0.04}_{-0.04}$	$^{+0.04}_{-0.04}$	-	$^{+0.04}_{-0.04}$
σ_E $\pm 20\%$	$^{+0.03}_{-0.03}$	$^{+0.03}_{-0.03}$	-	$^{+0.03}_{-0.03}$
σ_l $\pm 20\%$	$^{+0.04}_{-0.03}$	$^{+0.04}_{-0.03}$	-	$^{+0.04}_{-0.03}$
μVTX alignment	$^{+0.07}_{-0.07}$	$^{+0.07}_{-0.07}$	-	$^{+0.07}_{-0.07}$
Interaction point	$^{+0.01}_{-0.01}$	$^{+0.01}_{-0.01}$	-	$^{+0.01}_{-0.01}$
Total	$^{+0.11}_{-0.13}$	$^{+0.11}_{-0.12}$	$^{+0.06}_{-0.07}$	$^{+0.11}_{-0.11}$

Table 4: Summary of systematic errors.

three charged track decay vertices in τ decays. The effect of coherent radial shifts of the μVTX detector by ± 50 μm together with incoherent shifts of ± 100 μm was found to translate into a decay length error of ± 43 μm. We have conservatively assumed that any such effects might scale directly with the mass of the decaying particle because of the larger opening angle and therefore consider a variation of ± 130 μm. Possible effects due to variations in the size and position of the e^+e^- interaction point are expected to be similar to those found in τ decays, so we have used the same values as obtained in [18].

The resulting systematic uncertainties are summarized in table 4. We have combined all systematic errors in quadrature.

8 Conclusions

We have used a sample of about 130 (semi-)exclusive $B \to \overline{D}\ell^+$ decays to directly measure the B^0 and B^+ lifetimes. We find:

$$\tau^0 = 1.51^{+0.24+0.11}_{-0.23-0.13} \text{ ps}$$

$$\tau^+ = 1.52^{+0.29+0.11}_{-0.27-0.12} \text{ ps}$$

$$\tau^+/\tau^0 = 1.01^{+0.32+0.06}_{-0.24-0.07}$$

Our results confirm that the B^0 and B^+ lifetimes are similar. The measured average B lifetime, $\langle\tau\rangle = 1.51^{+0.16+0.11}_{-0.14-0.11}$ ps, is in good agreement with less direct measurements using inclusive leptons [1]. These results are also in agreement with similar measurements presented by the other LEP collaborations [19].

References

[1] ALEPH Collaboration, D. Buskulic *et al.*, *CERN-PPE/92-133* (1992);
DELPHI Collaboration, P. Abreu *et al.*, *Z. Phys.* **C53** (1992) 567;
L3 Collaboration, B. Adeva *et al.*, *Phys. Lett.* **B270** (1992) 111;
OPAL Collaboration, P. D. Acton *et al.*, *Phys. Lett.* **B274** (1992) 513.

[2] J. H. Kühn *et al.*, in Z physics at LEP 1, *CERN 89-08* (1989) ed. G. Altarelli *et al.*

[3] OPAL Collaboration, P. D. Acton *et al.*, *CERN-PPE/92-144* (1992), submitted to *Phys. Lett.*

[4] Preliminary OPAL results on the decay $\Lambda_b \to \Lambda_c^+ \ell^- \overline{\nu} \mathrm{X}$ were reported by X. C. Lou at the XXVI. International Conference on High Energy Physics, Dallas, August 1992.

[5] OPAL Collaboration, K. Ahmet *et al.*, *Nucl. Instrum. Methods* **A305** (1991) 275.

[6] P. P. Allport *et al.*, 'The OPAL Silicon Microvertex Detector', to be published in *Nucl. Instrum. Methods.*

[7] M. Hauschild *et al.*, *Nucl. Instrum. Methods* **A314** (1992) 74.

[8] OPAL Collaboration, P. D. Acton *et al.*, *Phys. Lett.* **B276** (1992) 379. More details can be found in: OPAL Collaboration, P. D. Acton *et al.*, *Z. Phys.* **C55** (1992) 191.

[9] OPAL Collaboration, G. Alexander *et al.*, *Z. Phys.* **C52** (1991) 175.

[10] J. Allison *et al.*, *Nucl. Instrum. Methods* **A317** (1992) 47.

[11] Particle Data Group, K. Hikasa *et al.*, *Phys. Rev* **D45** (1992) 1.

[12] CLEO Collaboration, F. Butler *et al.*, *CLNS 92-1143* (1992).

[13] ARGUS Collaboration, H. Albrecht *et al.*, *Phys. Lett.* **B197** (1987) 452;
ARGUS Collaboration, H. Albrecht *et al.*, *Phys. Lett.* **B229** (1989) 175;
ARGUS Collaboration, H. Albrecht *et al.*, *Phys. Lett.* **B275** (1992) 195;
CLEO Collaboration, D. Bortoletto *et al.*, *Phys. Rev. Lett.* **63** (1989) 1667.

[14] CLEO Collaboration, R. Fulton *et al.*, *Phys. Rev.* **D43** (1991) 651.

[15] ARGUS Collaboration, H. Albrecht *et al.*, *DESY 92-146* (1992).

[16] P. Colangelo, G. Nardulli and N. Paver, *Phys. Lett.* **B293** (1992) 207.

[17] J. L. Rosner, *Comm. Nucl. Part. Phys.* (1986) 109;
S. Godfrey and R. Kokoski, *Phys. Rev* **D43** (1991) 1679.

[18] OPAL Collaboration, P. D. Acton *et al.*, 'Measurement of the τ lifetime', to be submitted to *Phys. Lett.*

[19] DELPHI Collaboration, P. Abreu *et al.*, *CERN-PPE/92-174* (1992), submitted to *Z. Phys.* Preliminary results from ALEPH were reported by M. Feindt at the XXVI. International Conference on High Energy Physics, Dallas, August 1992, *CERN-PPE/92-174* (1992).

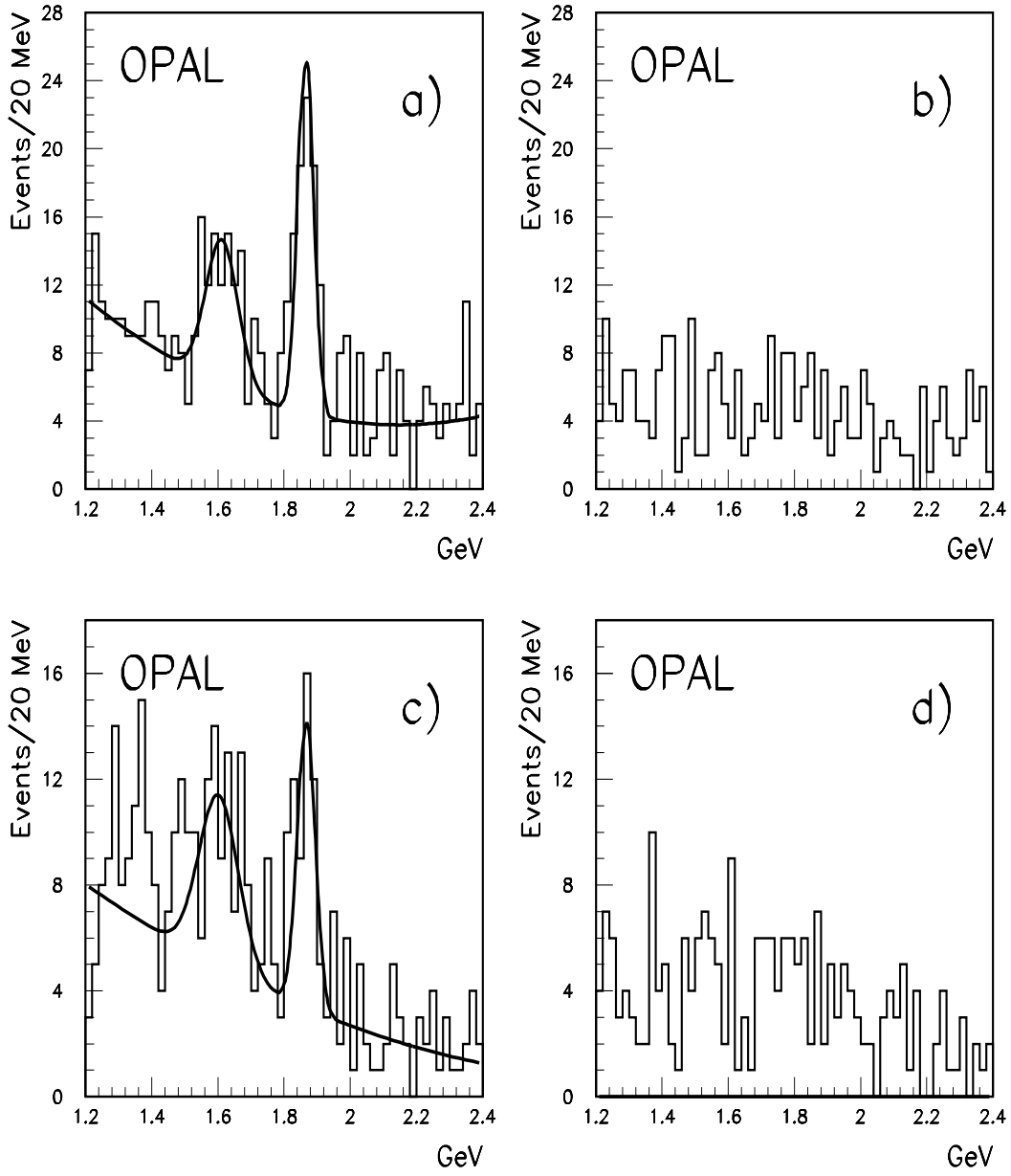

Figure 1: (a) Mass distribution of $K^-\pi^+$ combinations for events containing an ℓ^-. (b) Mass distribution of $K^-\pi^+$ combinations for events containing an ℓ^+. (c) Mass distribution of $K^-\pi^+\pi^+$ combinations for events containing an ℓ^-. (d) Mass distribution of $K^-\pi^+\pi^+$ combinations for events containing an ℓ^+. The curves shown are the results of fits using Gaussians plus polynomial background functions.

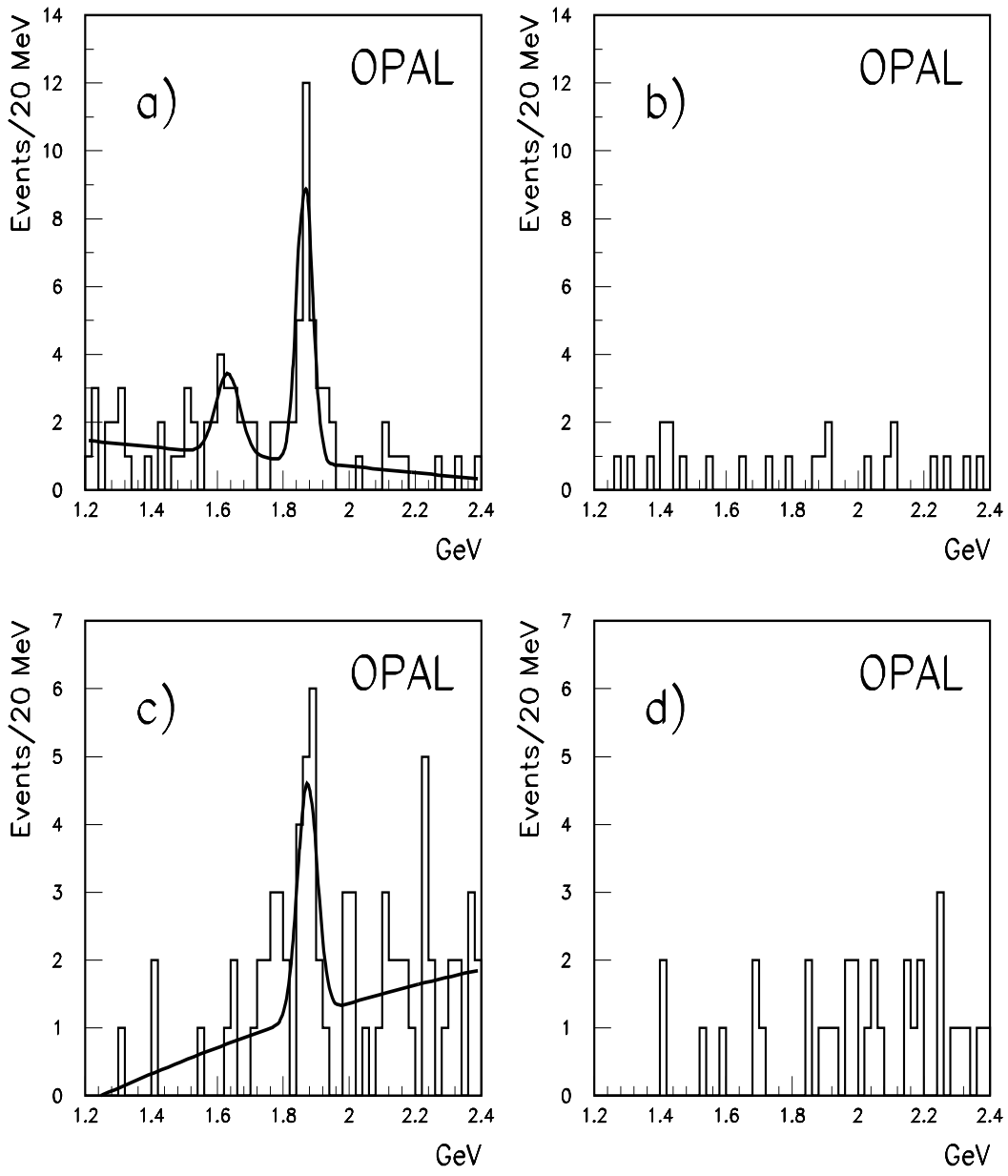

Figure 2: Mass distributions for events satisfying the D^{*+} selection cut. (a) Mass distribution of $K^-\pi^+$ combinations for events containing an ℓ^-. (b) Mass distribution of $K^-\pi^+$ combinations for events containing an ℓ^+. (c) Mass distribution of $K^-\pi^+\pi^+\pi^-$ combinations for events containing an ℓ^-. (d) Mass distribution of $K^-\pi^+\pi^+\pi^-$ combinations for events containing an ℓ^+. The curves shown are the results of fits using Gaussians plus polynomial background functions.

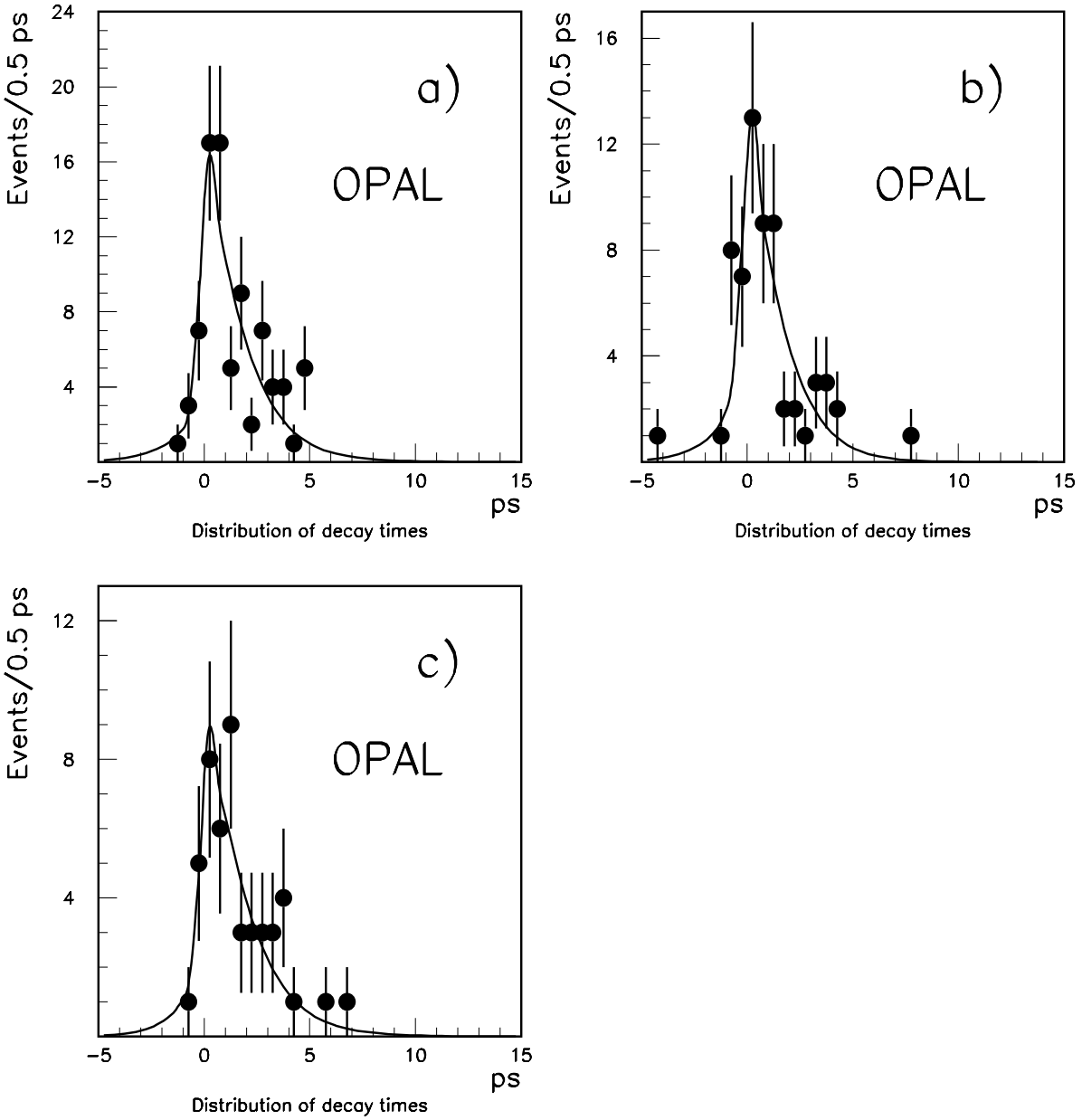

Figure 3: Decay time distributions for the different samples of $B \to \overline{D}\ell^+$ candidates. (a) $\overline{D}^0\ell^+$ events, (b) $D^-\ell^+$ events, and (c) $D^{*-}\ell^+$ events. The solid lines show the results of the maximum likelihood fit.

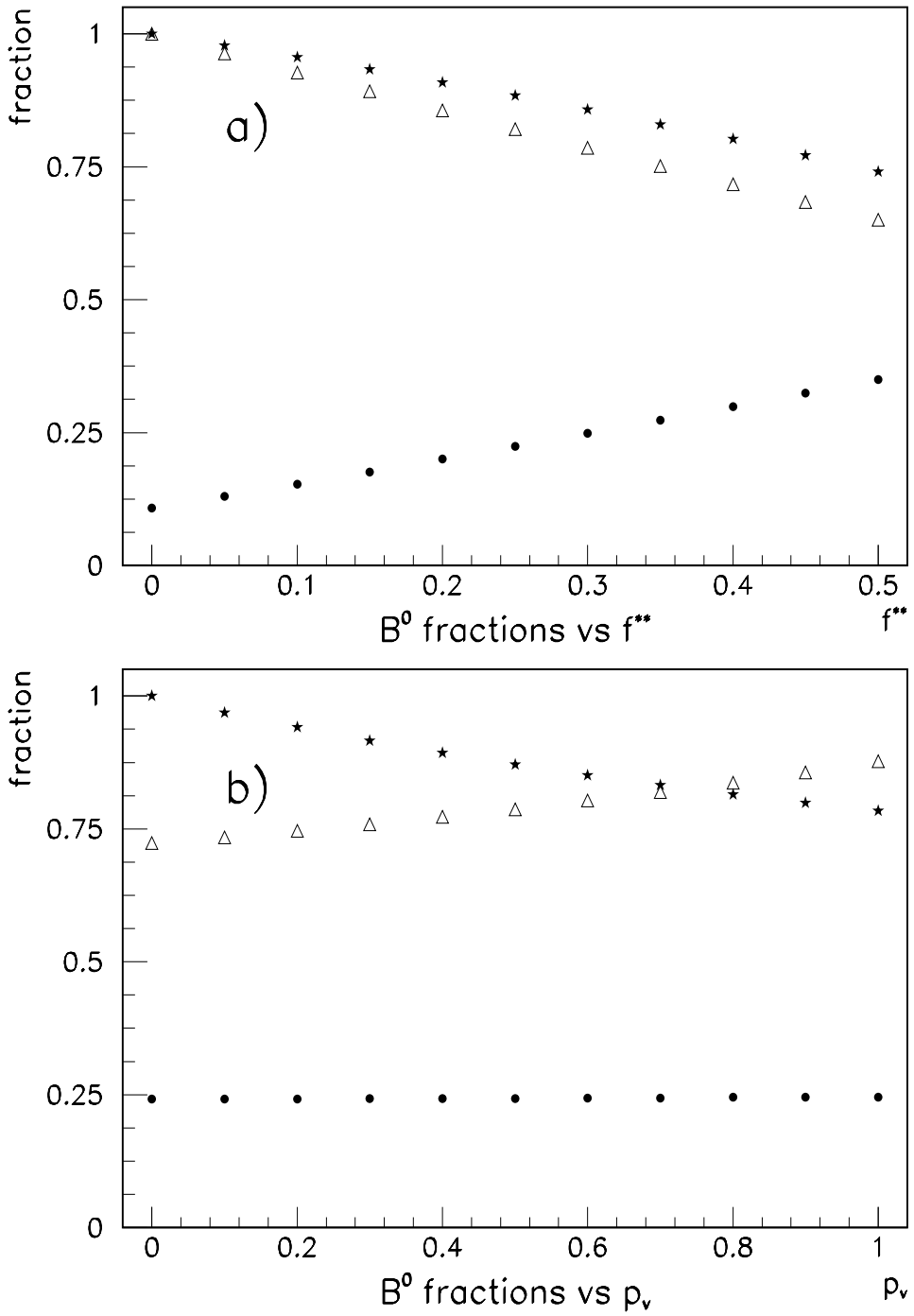

Figure 4: Predicted fraction of B^0 mesons in the samples of $\overline{D}^0\ell^+$ events ($\bullet$), $D^-\ell^+$ events ($\triangle$) and $D^{*-}\ell^+$ events ($\star$) as a function of (a) f^{**} with $p_v = 0.54$ and (b) p_v with $f^{**} = 0.36$.

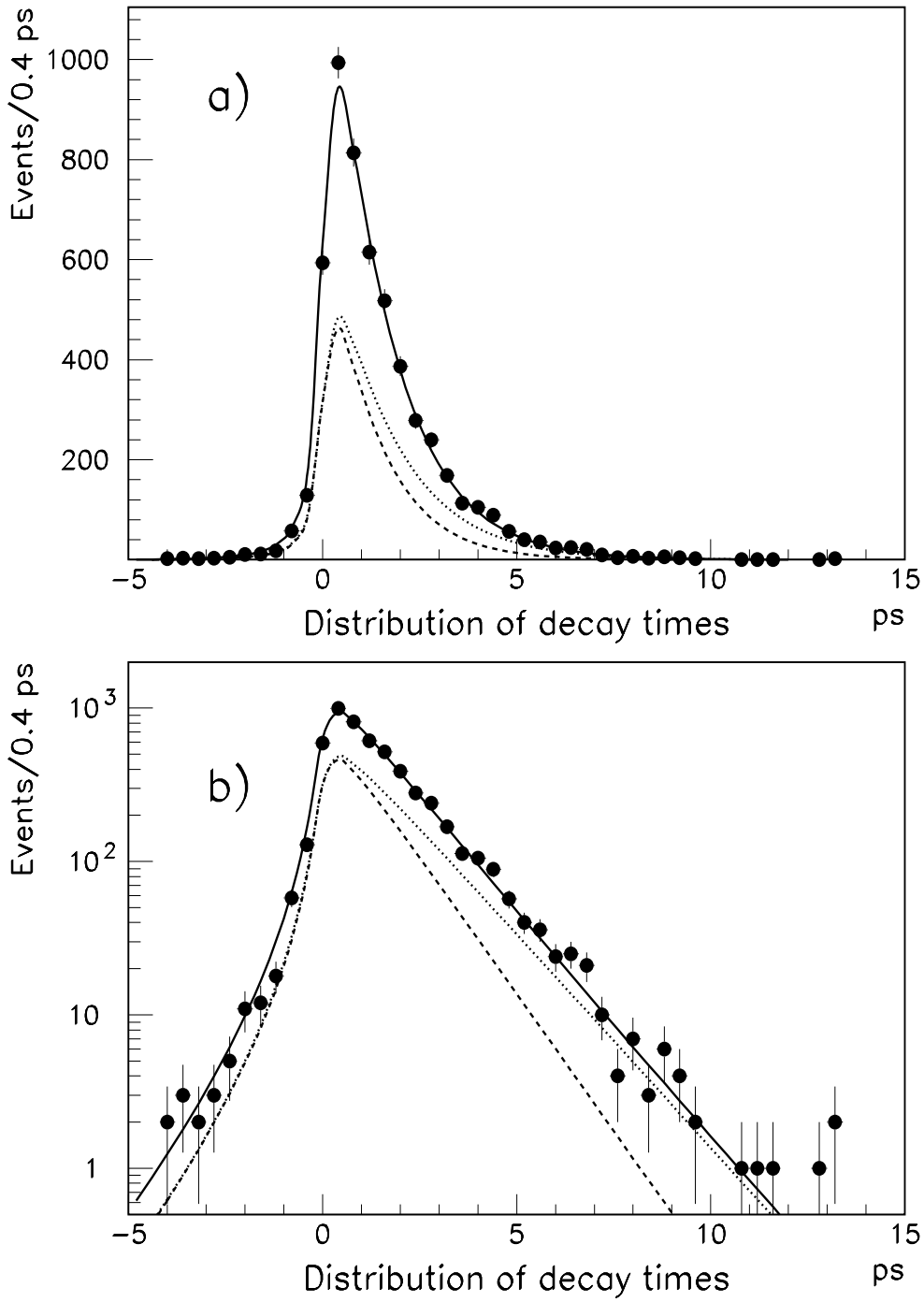

Figure 5: Reconstructed decay time distribution for a Monte Carlo sample with $\tau^0 = 1.2$ ps and $\tau^+ = 1.6$ ps. The solid line is the result of the maximum likelihood fit. The dashed and dotted lines indicate the fitted contributions from B^0 and B^+ respectively.

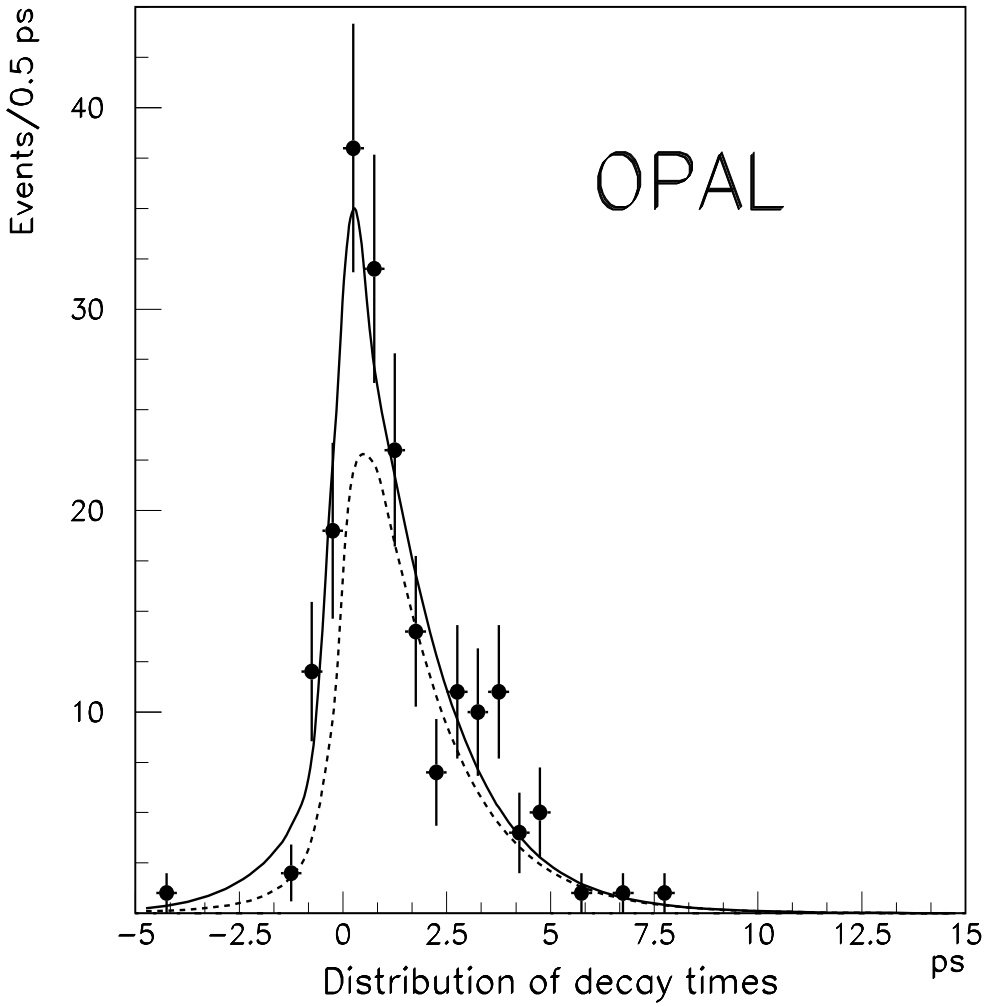

Figure 6: Reconstructed decay time distribution of the $B \to \overline{D}\ell^+$ candidates. The solid curve is the result of the maximum likelihood fit. The dotted curve shows the sum of the fitted contributions from the B^0 and B^+ events.